Proceedings of DETC2001
2001 ASME Design Engineering Technical Conferences
September 9-13, 2001, Pittsburgh, Pennsylvania, USA

DETC2001/VIB-21587

PERTURBATION SOLUTION FOR SECONDARY BIFURCATION IN THE QUADRATICALLY-DAMPED MATHIEU EQUATION

Deepak V. Ramani
Naval Undersea Warfare Center
Newport, RI 02841
e-mail: dvr3@cornell.edu

Richard H. Rand
Dept. of Theoretical & Applied Mechanics
Cornell University, Ithaca, NY 14853
e-mail: rhr2@cornell.edu

William L. Keith
Naval Undersea Warfare Center
Newport, RI 02841
e-mail: wlkeith@hotmail.com

ABSTRACT

This paper concerns the quadratically-damped Mathieu equation:

$$\ddot{x} + (\delta + \epsilon \cos t)\, x + \dot{x}\,|\dot{x}| = 0.$$

Numerical integration shows the existence of a secondary bifurcation in which a pair of limit cycles come together and disappear (a saddle-node bifurcation of limit cycles). In $\delta - \epsilon$ parameter space, this secondary bifurcation appears as a curve which emanates from one of the transition curves of the linear Mathieu equation for $\epsilon \approx 1.5$. The bifurcation point along with an approximation for the bifurcation curve is obtained by a perturbation method which uses Mathieu functions rather than the usual sines and cosines.

INTRODUCTION

The Mathieu equation

$$\ddot{x} + (\delta + \epsilon \cos t)\, x = 0 \tag{1}$$

is a well-known example of a linear differential equation with periodic coefficients. The stability properties of the Mathieu equation may be obtained by the use of Floquet theory; see (Stoker, 1950). A survey of some of nonlinear variations of the Mathieu equation has been presented in (Nayfeh and Mook, 1979).

The quadratically-damped Mathieu equation,

$$\ddot{x} + (\delta + \epsilon \cos t)\, x + \dot{x}\,|\dot{x}| = 0, \tag{2}$$

which is studied here, has application to the dynamics of passive towed arrays in submarines. The physical application and the derivation of the equation has been detailed in (Rand et al., 2000a) and (Rand et al., 2000b). In addition to deriving the quadratically-damped Mathieu equation, the previous works carried out a linear stability analysis as well as a small-ϵ nonlinear stability analysis via the method of averaging. These works also contained an incomplete analytical treatment of the secondary bifurcation. The objective of the present work is to complete the analytical treatment of the secondary bifurcation, to determine the nature of the bifurcation, and to approximate the bifurcation curve.

LINEAR STABILITY AND SMALL ϵ RESULTS

Equation (2) admits the exact solution $x \equiv 0$. The stability of this solution is governed by the linear Mathieu equation, Equation (1). The origin is considered **stable** if all solutions of Equation (1) are bounded, and **unstable** if an unbounded solution exists. The stability treatment of Equation (1) demonstrates the existence of regions in the δ-ϵ plane, called tongues, which emanate from the δ-axis at points $\delta = n^2/4$, where $n = 0, 1, 2, 3, \cdots$ (Stoker, 1950). Inside the tongues, the origin is unstable, while outside the

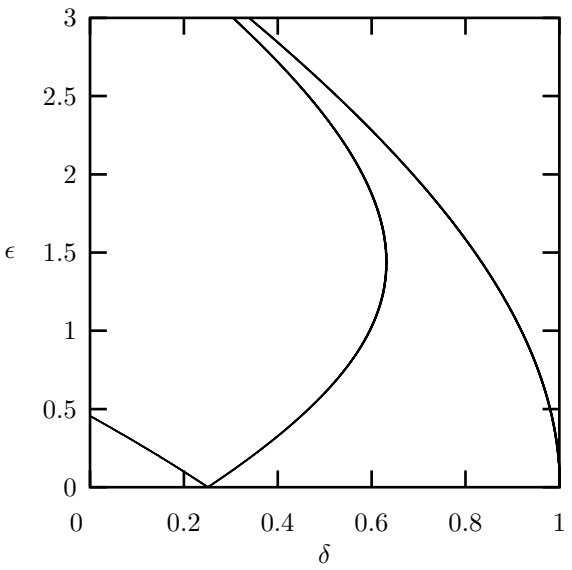

Figure 1. Transition curves of the linear Mathieu equation

tongues, the origin is stable. The tongues of instability are said to be bounded by **transition curves.** Because the linear Mathieu equation governs the stability of the origin in the quadratically-damped Mathieu equation, the transition curves of the linear Mathieu equation represent bifurcation curves for the quadratically-damped Mathieu equation.

Although the linear stability analysis predicts unbounded growth inside the tongues, this is not the case in the nonlinear equation (2). Inside the tongues, the nonlinear damping in Equation (2) balances the parametric resonance, leading to the existence of a periodic motion inside the tongues. The method of averaging (see (Rand, 1994)) can be used both to show that periodic motions exist inside the instability tongues, and to obtain an approximation to these periodic motions, valid for small ϵ. The details of this calculation are given in (Rand et al., 2000b). These results predict that at points lying inside the tongue emanating from $\delta = 1/4, \epsilon = 0$, equation (2) exhibits an attractive 2:1 subharmonic motion having period 4π. For this reason the points lying inside this tongue will be referred to as the 2:1 region. Similarly, at points lying inside the tongue emanating from $\delta = 1, \epsilon = 0$, equation (2) is predicted to exhibit a pair of attractive 1:1 periodic motions, each having period 2π. This region will be referred to as the 1:1 region.

NUMERICAL DETERMINATION OF THE SECONDARY BIFURCATION

Numerical explorations of the nonlinear quadratically-damped Mathieu equation (2) may be accomplished by generating a Poincaré map corresponding to a surface of section $t = 0 \bmod 2\pi$. Using this technique, a variety of periodic motions are observed, depending upon where we are in the $\delta - \epsilon$ parameter plane. Figure 2 shows schematically the different Poincaré map portraits that are exhibited by equation (2). In these diagrams, periodic motions appear as fixed points.

We may summarize the features displayed in Figure 2 as follows: Outside the instability regions, the origin is always stable, as indicated by a lone spiral to the origin. Inside the instability regions, the origin is unstable, as indicated by a saddle-like x at the origin. Inside the 2:1 region the two spiral singularities in the Poincaré map represent a single period 4π motion, whereas in the 1:1 region they represent two period 2π motions. As the transition curves are crossed into 1:1 region or into the 2:1 region below point P, a supercritical pitchfork bifurcation occurs, and two new stable singular points are created in the Poincaré map, while the origin itself becomes unstable. As the 2:1 region is exited above point P into the region marked B (see Figure 2), a subcritical pitchfork bifurcation occurs. In this case, the origin becomes stable and an unstable 2:1 subharmonic periodic motion is created. As region B is exited into region C, the 1:1 transition curve is crossed, and the expected supercritical pitchfork bifurcation curve takes place at the origin. The origin once more becomes unstable, while two stable period 2π motions are born out of the origin.

Perhaps the most interesting feature displayed in Figure 2 corresponds to what happens when we move from either of regions B or C downward across the nearly-straight line bifurcation curve emanating from point P. In this case the two outermost periodic orbits – the stable and unstable period 4π orbits – are destroyed in a saddle-node bifurcation. It is seen that this saddle-node bifurcation does not take place at the origin. **It is the goal of this work to obtain an analytic approximation for this curve on which this secondary bifurcation takes place.**

ANALYTICAL DETERMINATION OF THE SECONDARY BIFURCATION

In this section, the secondary bifurcation is investigated by a perturbation method applied at the point P. In order to cast Equation (2) in the proper format, we scale it to

$$\ddot{x} + (\delta + \epsilon \cos t)\, x + \mu \dot{x} \left|\dot{x}\right| = 0, \tag{3}$$

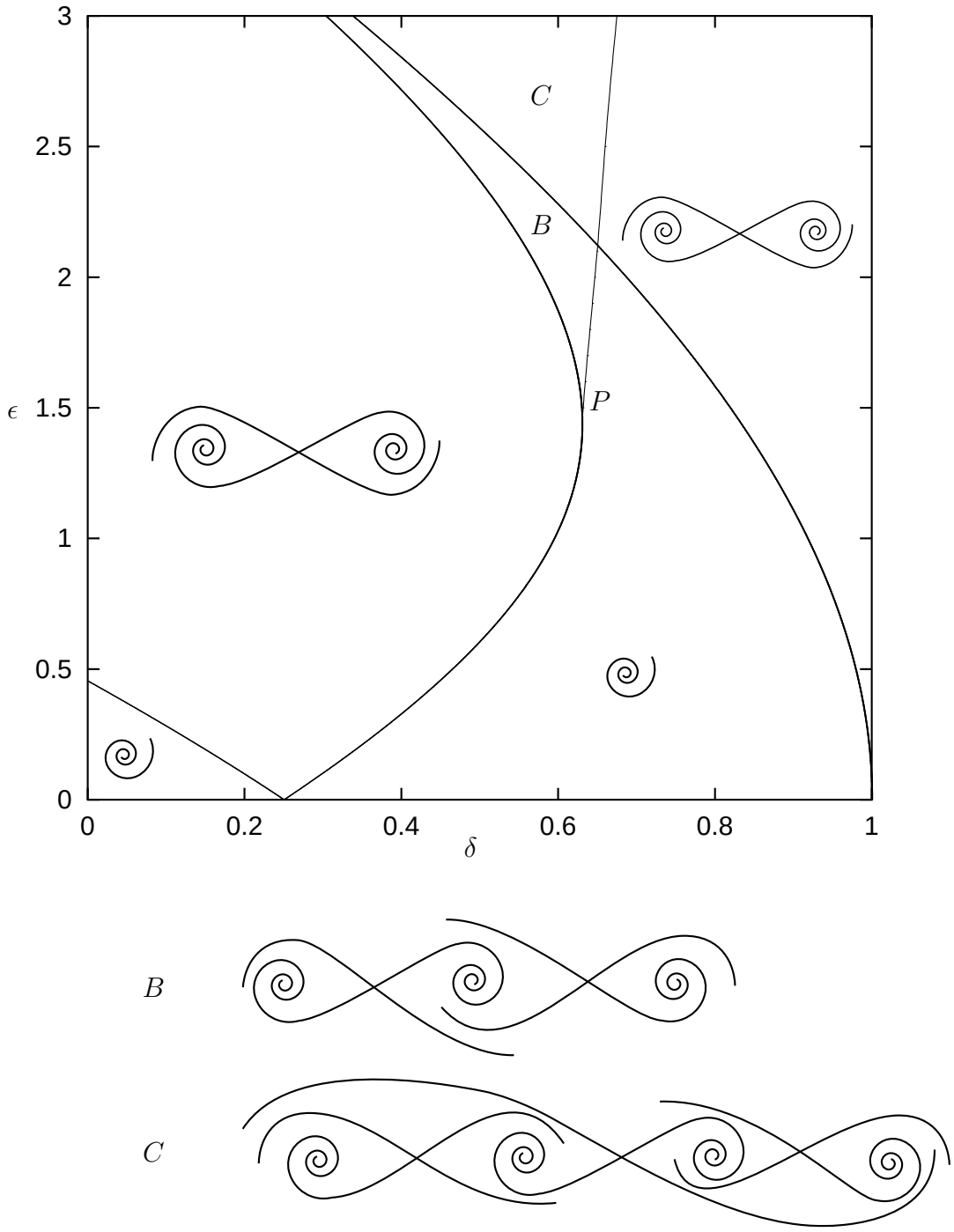

Figure 2. Phase portraits of the Poincaré Map in the different regions of the parameter plane in the quadratic Mathieu equation.

where the parameter μ is assumed to be small. We further expand δ and x as follows

$$x = x_0 + \mu x_1 + \mu^2 x_2 + \mu^3 x_3 + \mu^4 x_4 + \mu^5 x_5 + \cdots \quad (4)$$

$$\delta = \delta_0 + \mu\delta_1 + \mu^2\delta_2 + \mu^3\delta_3 + \mu^4\delta_4 + \mu^5\delta_5 + \cdots, \quad (5)$$

and further introduce the parameter ϵ_1 defined by

$$\epsilon = \epsilon_0 + \mu\epsilon_1. \quad (6)$$

The quantities δ_0 and ϵ_0 refer to the location of P. The parameter ϵ_1 measures the deviation of ϵ from ϵ_0 at P. Equations (3) – (6) represent a perturbation expansion off of the linear Mathieu equation. Because of this, the solution of the unperturbed equation will involve Mathieu functions. The perturbation functions x_i are each required to be periodic.

When Equations (4) – (6) are inserted into Equation (3) and terms are collected in powers of μ, the perturbation equations are

$$Lx_0 = 0 \quad (7)$$

$$Lx_1 = -\left(\delta_1 + \epsilon_1\cos t\right)x_0 - \frac{dx_0}{dt}\left|\frac{dx_0}{dt}\right| \quad (8)$$

$$Lx_2 = -\delta_2 x_0 - \left(\delta_1 + \epsilon_1\cos t\right)x_1 - 2\frac{dx_1}{dt}\left|\frac{dx_0}{dt}\right| \quad (9)$$

$$\begin{aligned} Lx_3 = &-\delta_3 x_0 - \delta_2 x_1 - \left(\delta_1 + \epsilon_1\cos t\right)x_2 \\ &- 2\frac{dx_2}{dt}\left|\frac{dx_0}{dt}\right| - \left(\frac{dx_1}{dt}\right)^2 \operatorname{sgn}\left[\frac{dx_0}{dt}\right] \end{aligned} \quad (10)$$

$$\begin{aligned} Lx_4 = &-\delta_4 x_0 - \delta_3 x_1 - \delta_2 x_2 - \left(\delta_1 + \epsilon_1\cos t\right)x_3 \\ &- 2\frac{dx_3}{dt}\left|\frac{dx_0}{dt}\right| - 2\operatorname{sgn}\left[\frac{dx_0}{dt}\right]\frac{dx_1}{dt}\frac{dx_2}{dt} \\ &- \frac{1}{3}\left(\frac{dx_1}{dt}\right)^3 \delta\left(\frac{dx_0}{dt}\right) \end{aligned} \quad (11)$$

$$\begin{aligned} Lx_5 = &-\delta_5 x_0 - \delta_4 x_1 - \delta_3 x_2 - \delta_2 x_3 \\ &- \left(\delta_1 + \epsilon_1\cos t\right)x_4 \\ &- 2\frac{dx_4}{dt}\left|\frac{dx_0}{dt}\right| - 2\frac{dx_1}{dt}\frac{dx_3}{dt}\operatorname{sgn}\left[\frac{dx_0}{dt}\right] \\ &- \left(\frac{dx_2}{dt}\right)^2 \operatorname{sgn}\left[\frac{dx_0}{dt}\right] \\ &- \frac{1}{12}\left(\frac{dx_1}{dt}\right)^4 \delta'\left(\frac{dx_0}{dt}\right) \\ &- \left(\frac{dx_1}{dt}\right)^2 \frac{dx_2}{dt}\delta\left(\frac{dx_0}{dt}\right), \end{aligned} \quad (12)$$

where

$$L \equiv \frac{d^2}{dt^2} + \left(\delta_0 + \epsilon_0\cos t\right) \quad (13)$$

is defined as the Mathieu operator, and where sgn is the signum function and δ is the Dirac-δ function. The signum and Dirac-δ functions arise from the derivatives of the absolute value term in Equation (3).

The first perturbation equation, Equation (7), is the linear Mathieu equation. Because P is on the right-hand transition curve of the 2:1 instability tongue, Equation (7) has as its solution the odd Mathieu function of period 4π (Stoker, 1950). Therefore

$$x_0 = Af_1, \quad (14)$$

where A is a constant that represents the amplitude of a periodic motion, and f_1 denotes the Mathieu function. In this case, the second linearly independent solution of Mathieu's equation is not used because it is not periodic. In order to simplify what follows we introduce the notational convention that **any function labeled f_i is an odd function, whereas any function labeled g_i is an even function.**

By inserting Equation (14) into Equation (8) the following equation for x_1 is obtained

$$Lx_1 = -\left(\delta_1 + \epsilon_1\cos t\right)Af_1 - A^2\dot{f}_1\left|\dot{f}_1\right|. \quad (15)$$

Because A represents the amplitude of a motion, it may be thought of as positive. The constant δ_1 is chosen to eliminate secular terms. The secular terms are eliminated by using the Fredholm alternative theorem which states that for a periodic solution to exist for

$$Lx = F, \quad (16)$$

the function F must be orthogonal to the null space of the adjoint operator L^*. In this case, L is self-adjoint, and its null space is spanned by the function f_1. The orthogonality condition is expressed as

$$\int_0^{4\pi} f_1 F \; dt = 0. \quad (17)$$

The Fredholm condition is

$$\begin{aligned} \int_0^{4\pi} Af_1 H_1 \; dt = &-\int_0^{4\pi} \left(\delta_1 + \epsilon_1\cos t\right)A^2 f_1^2 \; dt \\ &-\int_0^{4\pi} A^3 f_1\dot{f}_1\left|\dot{f}_1\right| \; dt = 0. \end{aligned} \quad (18)$$

The term $-\int_0^{4\pi}(\delta_1+\epsilon_1\cos t)A^2 f_1^2\ dt$ in Equation (18) cannot be further simplified. In the term $-\int_0^{4\pi} A^3 f_1 \dot{f}_1 \left|\dot{f}_1\right|\ dt$, f_1 is an odd function and therefore $\dot{f}_1$ is an even function. Thus, the integrand in the second term is an odd function that is periodic over an interval of 4π. Since the integral of an odd function over a periodic interval is 0, this term vanishes, leaving

$$\delta_1 \int_0^{4\pi} f_1^2\ dt + \epsilon_1 \int_0^{4\pi} f_1^2 \cos t\ dt = 0, \tag{19}$$

or

$$\frac{\epsilon_1}{\delta_1} = -\frac{\int_0^{4\pi} f_1^2\ dt}{\int_0^{4\pi} f_1^2 \cos t\ dt}. \tag{20}$$

However, the only nonlinear term in the analysis to this point has vanished without having an effect on the integration. Therefore, the relationship between ϵ_1 and δ_1 derived in Equation (20) must also hold for the linear Mathieu equation. The ratio of ϵ_1 to δ_1 is the local slope of the transition curve near the point (δ_0, ϵ_0). Since P is taken to be the point where the transition curve has infinite slope, this forces $\delta_1 = 0$. From Equation (20) this is equivalent to requiring

$$\int_0^{4\pi} f_1^2 \cos t\ dt = 0, \tag{21}$$

at (δ_0, ϵ_0). This requirement provides an analytical condition for (δ_0, ϵ_0), the location of point P on the transition curve.

By substituting $\delta_1 = 0$ back into Equation (15), the equation on x_1 is now formulated in a solvable way

$$Lx_1 = -\epsilon_1 A f_1 \cos t - A^2 \dot{f}_1 \left|\dot{f}_1\right|. \tag{22}$$

The first term on the right hand side of Equation (22) is an odd term, whereas the second term is an even term. By linearity these may be treated independently, and the sum of their individual particular solutions may be used to solve the full equation. Therefore, the functions f_2 and g_1 are defined by

$$Lf_2 = -f_1 \cos t \tag{23}$$

$$Lg_1 = -\dot{f}_1 \left|\dot{f}_1\right|. \tag{24}$$

The solution to the full equation (22) is then

$$x_1 = A\epsilon_1 f_2 + A^2 g_1. \tag{25}$$

For the most general periodic solution, an arbitrary multiple of f_1 could be added to the solution for x_1. In fact, because $Lf_1 = 0$, arbitrary multiples of f_1 could be added to any of the odd functions that arise from the perturbation method. However, it is shown in (Ramani, 2001) that the results of the method are independent of the addition of multiples of f_1. Therefore, no multiple of f_1 will be added to any of the solutions, in order to ease the algebra. Note that an arbitrary multiple of f_1 cannot be added to any of the g_i. This is because the g_i are required to be even functions. This property would be destroyed by adding multiples of the odd function f_1.

By continuing in a similar fashion, the second Fredholm condition becomes

$$\begin{aligned} &A^2\delta_2 \int_0^{4\pi} f_1^2\ dt + A^2\epsilon_1 \int_0^{4\pi} f_1 f_2 \cos t\ dt \\ &+ A^3\epsilon_1 \int_0^{4\pi} f_1 \left(g_1 \cos t + 2\dot{f}_2 \left|\dot{f}_1\right|\right)\ dt \\ &+ 2A^4 \int_0^{4\pi} f_1 \left|\dot{f}_1\right| \dot{g}_1\ dt = 0, \end{aligned} \tag{26}$$

which can be solved to yield

$$\begin{aligned} \delta_2 &= -\epsilon_1 \frac{\int_0^{4\pi} f_1 f_2 \cos t\ dt}{\int_0^{4\pi} f_1^2 dt} - 2A^2 \frac{\int_0^{4\pi} f_1 \left|\dot{f}_1\right| \dot{g}_1\ dt}{\int_0^{4\pi} f_1^2 dt} \\ &\equiv k_1\epsilon_1 + 2k_2 A^2, \end{aligned} \tag{27}$$

where

$$k_1 = -\frac{\int_0^{4\pi} f_1 f_2 \cos t\ dt}{\int_0^{4\pi} f_1^2 dt} \tag{28}$$

$$k_2 = -\frac{\int_0^{4\pi} f_1 \left|\dot{f}_1\right| \dot{g}_1\ dt}{\int_0^{4\pi} f_1^2 dt}, \tag{29}$$

are constants that need to be computed numerically.

Substituting Equation (27) back into the last of Equation (9), a new equation on x_2 is obtained:

$$\begin{aligned} Lx_2 = &- A\epsilon_1^2 (f_1 + f_2 \cos t) \\ &- A^2\epsilon_1 \left(g_1 \cos t + 2\dot{f}_2 \left|\dot{f}_1\right|\right) \\ &- 2A^3 \left(f_1 + \left|\dot{f}_1\right| \dot{g}_1\right). \end{aligned} \tag{30}$$

Each of the three terms on the right hand side of (30) is either even or odd, and so the solution for x_2 consists of three terms

$$x_2 = A\epsilon_1^2 f_3 + A^2\epsilon_1 g_2 + 2A^3 f_4, \tag{31}$$

where

$$Lf_3 = -k_1 f_1 - f_2 \cos t \tag{32}$$

$$Lg_2 = -g_1 \cos t - 2\dot{f}_2 \left|\dot{f}_1\right| \tag{33}$$

$$Lf_4 = -k_2 f_1 - \dot{g}_1 \left|\dot{f}_1\right|. \tag{34}$$

This procedure is continued at each higher order of μ. At each stage, the latest δ_i is obtained from the Fredholm condition. Using δ_i, the differential equation on x_i is solved. At each stage, new constants k_i are also introduced. The bifurcation curve is determined by the values of δ_i and k_i. For that reason, they are given here. The definitions of the auxiliary functions f_i and g_i as well as the solutions to Equations (7) – (11) are given in the Appendix.

The δ_i are

$$\delta_1 = 0 \tag{35}$$

$$\delta_2 = k_1\epsilon_1^2 + 2k_2 A^2 \tag{36}$$

$$\delta_3 = k_3\epsilon_1^2 + k_4 A^2\epsilon_1 \tag{37}$$

$$\delta_4 = k_5 A^4 + k_6 A^2\epsilon_1^2 + k_7\epsilon_1^4 \tag{38}$$

$$\begin{aligned}\delta_5 = {} & \epsilon_1^5 k_8 + A^2\epsilon_1^3 k_9 + A^3\epsilon_1^3 k_{10} + A^4\epsilon_1 k_{11} \\ & + A^4\epsilon_1^3 k_{12} + A^5\epsilon_1 k_{13} + A^6\epsilon_1 k_{14},\end{aligned} \tag{39}$$

where

$$k_1 = -\frac{\int_0^{4\pi} f_1 f_2 \cos t \; dt}{\int_0^{4\pi} f_1^2 \; dt} \tag{40}$$

$$k_2 = -\frac{\int_0^{4\pi} f_1 \dot{g}_1 \left|\dot{f}_1\right| \; dt}{\int_0^{4\pi} f_1^2 \; dt} \tag{41}$$

$$k_3 = -\frac{\int_0^{4\pi} k_1 f_1 f_2 + f_1 f_2 \cos t \; dt}{\int_0^{4\pi} f_1^2 \; dt} \tag{42}$$

$$\begin{aligned}k_4 = {} & -\frac{\int_0^{4\pi} 2k_2 f_1 f_2 + 2f_1 f_4 \cos t + 2f_1 \dot{g}_2 \left|\dot{f}_1\right| \; dt}{\int_0^{4\pi} f_1^2 \; dt} \\ & - \frac{\int_0^{4\pi} 2f_1 \dot{f}_2 \dot{g}_1 \; \mathrm{sgn}\dot{f}_1 \; dt}{\int_0^{4\pi} f_1^2 \; dt}\end{aligned} \tag{43}$$

$$k_5 = -\frac{\int_0^{4\pi} 4f_1 \dot{f}_4 \dot{g}_1 \; \mathrm{sgn}\dot{f}_1 + 2f_1 \dot{g}_4 \left|\dot{f}_1\right| \; dt}{\int_0^{4\pi} f_1^2 \; dt} \tag{44}$$

$$\begin{aligned}k_6 = {} & -\frac{\int_0^{4\pi} 2f_1 \dot{f}_3 \dot{g}_1 \; \mathrm{sgn}\dot{f}_1 + 2f_1 \dot{f}_2 \dot{g}_2 \; \mathrm{sgn}\dot{f}_1 \; dt}{\int_0^{4\pi} f_1^2 \; dt} \\ & - \frac{\int_0^{4\pi} 2f_1 \dot{g}_3 \left|\dot{f}_1\right| + 2k_1 f_1 f_4 + 2k_2 f_1 f_3 \; dt}{\int_0^{4\pi} f_1^2 \; dt}\end{aligned} \tag{45}$$

$$k_7 = -\frac{\int_0^{4\pi} k_1 f_1 f_3 + f_1 f_g \cos t + k_3 f_1 f_2 \; dt}{\int_0^{4\pi} f_1^2 \; dt} \tag{46}$$

$$k_8 = -\frac{\int_0^{4\pi} f_1 \left(k_7 f_2 + k_3 f_3 + k_1 f_6 + f_7 \cos t\right) \; dt}{\int_0^{4\pi} f_1^2 dt} \tag{47}$$

$$\begin{aligned}k_9 = {} & -\frac{\int_0^{4\pi} f_1 \left(k_6 f_2 + k_4 f_3 + 2k_3 f_4 + 2k_2 f_6\right) \; dt}{\int_0^{4\pi} f_1^2 dt} \\ & - \frac{\int_0^{4\pi} f_1 \left(k_5 f_5 + 2\dot{g}_5 \left|\dot{f}_1\right|\right) \; dt}{\int_0^{4\pi} f_1^2 dt} \\ & - \frac{\int_0^{4\pi} f_1 \left(2\dot{f}_2 \dot{g}_3 \,\mathrm{sgn}\, \dot{f}_1 + 2\dot{f}_3 \dot{g}_2 \,\mathrm{sgn}\, \dot{f}_1\right) \; dt}{\int_0^{4\pi} f_1^2 dt} \\ & - \frac{\int_0^{4\pi} f_1 \left(2\dot{f}_6 \dot{g}_1 \,\mathrm{sgn}\, \dot{f}_1 + f_8 \cos t\right) \; dt}{\int_0^{4\pi} f_1^2 dt}\end{aligned} \tag{48}$$

$$k_{10} = -\frac{2}{3}\frac{\int_0^{4\pi} f_1 \left(\dot{g}_7 \left|\dot{f}_1\right| + f_{11} \cos t\right) \; dt}{\int_0^{4\pi} f_1^2 dt} \tag{49}$$

$$\begin{aligned}k_{11} = {} & -\frac{\int_0^{4\pi} f_1 \left(k_5 f_2 + 2k_4 f_4 + 2k_2 f_5\right) \; dt}{\int_0^{4\pi} f_1^2 dt} \\ & - \frac{\int_0^{4\pi} f_1 \left(2\dot{g}_6 \left|\dot{f}_1\right| + 2\dot{f}_2 \dot{g}_4 \,\mathrm{sgn}\, \dot{f}_1\right) \; dt}{\int_0^{4\pi} f_1^2 dt} \\ & - \frac{\int_0^{4\pi} f_1 \left(4\dot{f}_4 \dot{g}_2 \,\mathrm{sgn}\, \dot{f}_1 + 2\dot{f}_5 \dot{g}_1 \,\mathrm{sgn}\, \dot{f}_1 + f_9 \cos t\right) \; dt}{\int_0^{4\pi} f_1^2 dt}\end{aligned} \tag{50}$$

$$k_{12} = -\frac{1}{3}\frac{\int_0^{4\pi} f_1 \dot{f}_2^3 \dot{g}_1 \delta'\left(\dot{f}_1\right) \; dt}{\int_0^{4\pi} f_1^2 dt} \tag{51}$$

$$k_{13} = -\frac{\int_0^{4\pi} f_1 \left(2\dot{g}_8 \left|\dot{f}_1\right| + \frac{1}{3} f_{10} \cos t\right) \; dt}{\int_0^{4\pi} f_1^2 dt} \tag{52}$$

$$k_{14} = -\frac{1}{3}\frac{\int_0^{4\pi} f_1 \dot{f}_2 \dot{g}_1^3 \delta'\left(\dot{f}_1\right) \; dt}{\int_0^{4\pi} f_1^2 dt}. \tag{53}$$

Table 1. Values of k_i

k_1	-0.176795720204351	k_8	-0.005343518899145
k_2	0.000449147391502	k_9	0.041196711700806
k_3	0.023845390107660	k_{10}	0.000000000000001
k_4	0.059627911982873	k_{11}	0.243420338228478
k_5	0.008051597731526	k_{12}	0.024121956135593
k_6	0.133978124987812	k_{13}	0.000000000000000
k_7	0.008726800055536	k_{14}	0.003191162023248

Numerical solution of the perturbation Equations (7) – (11) yields the functions f_i and g_i (see Appendix) and then the values of the k_i may be found by numerical quadrature, see Table 1. Because the f_i and the g_i are required to be periodic functions, their initial conditions need to be chosen carefully. A shooting procedure was used first to locate δ_0 and ϵ_0, and then to obtain the initial conditions for the g_i. The shooting method returned $\delta_0 = 0.630420248517023$ and $\epsilon_0 = 1.438618533234416$ in double precision, in agreement with values obtained by direct numerical integration of Equation (2).

Substituting Equations (35) – (39) into Equation (5), the following expression for δ is obtained:

$$\begin{aligned}\delta =&\delta_0 + \epsilon_1 k_{14} A^6 + \left(\epsilon_1 k_{11} + \epsilon_1^3 k_{12} + k_5\right) A^4 \\ &+ \left(2k_2 + k_4\epsilon_1 + k_6\epsilon_1^2 + k_9\epsilon_1^3\right) A^2 \\ &+ \left(k_1\epsilon_1^2 + k_3\epsilon_1^3 + k_7\epsilon_1^4 + k_8\epsilon_1^5\right).\end{aligned} \tag{54}$$

This equation relates a given value of δ and ϵ_1 to the predicted amplitude A of the newly bifurcated unstable 2:1 subharmonic 4π-periodic orbit. As a check on all the perturbation calculations, we may use this equation to generate a value of A with which we may compare the perturbation expression for $x(t)$, that is, Equation (4) supplemented by the expressions in the Appendix and the values of the k_i in Table 1, with the results of direct numerical integration of Equation (2). To obtain a comparison, a method of numerically generating the unstable orbit is needed. This can be done by starting the integration near the stable manifold of the unstable orbit. If the initial condition is close enough to the stable manifold, the system will spend enough time near the unstable orbit to obtain a good approximation of it.

Figures 3 and 4 offer a comparison between the predicted unstable periodic orbit obtained from the perturbation method (dashed) and from numerical integration

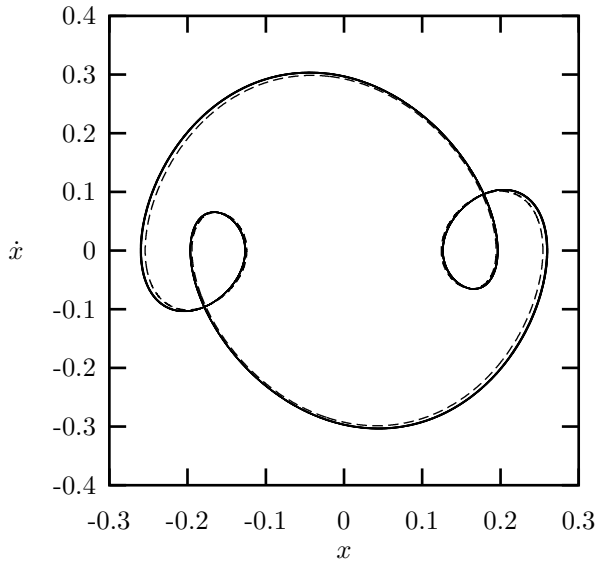

Figure 3. Comparison of numerical and analytical approximations of unstable periodic orbit in the phase plane. Analytical approximation is dashed, numerical integration is solid. Here $\delta = 0.6305$, $\epsilon = 1.47$ and $A = 0.2542$. $\delta_0 \approx 0.6304$, and $\epsilon_0 \approx 1.4386$.

(solid) for $\delta = 0.6305$ and $\epsilon = 1.47$. For these values of the parameters, Equation (54) predicts $A \approx 0.2542$. Figure 3 shows a phase portrait of the system, while Figure 4 shows the time history of the system. For these values of δ and ϵ, the agreement between the analytical approximation and the numerical integration is quite good. For comparison, the location of P was determined to be about $\delta_0 \approx 0.6304$ and $\epsilon_0 \approx 1.4386$.

As the value of δ is increased away from the transition curve and towards the secondary bifurcation curve, the agreement between the analytical and numerical solutions worsens. Figures 5 and 6 show the approximations for $\delta = 0.631$ and $\epsilon = 1.47$, with the bifurcation point P located at $\delta_0 \approx 0.6304$ and $\epsilon_0 \approx 1.4386$. Despite the small change in δ there is a marked change in the agreement. These figures suggest that the power series may not converge close to the bifurcation curve. The lack of accuracy could be due to either the number of terms taken being too small or the radius of convergence of the series not being large enough to reach the bifurcation curve. In the former case, more terms could be added, but the computational difficulties increase considerably with each step. In the latter case, the power series expansion will not give reasonable agreement near the bifurcation curve, no matter how many terms are taken.

With these convergence problems in mind, we now proceed to attempt to obtain an analytical expression for the

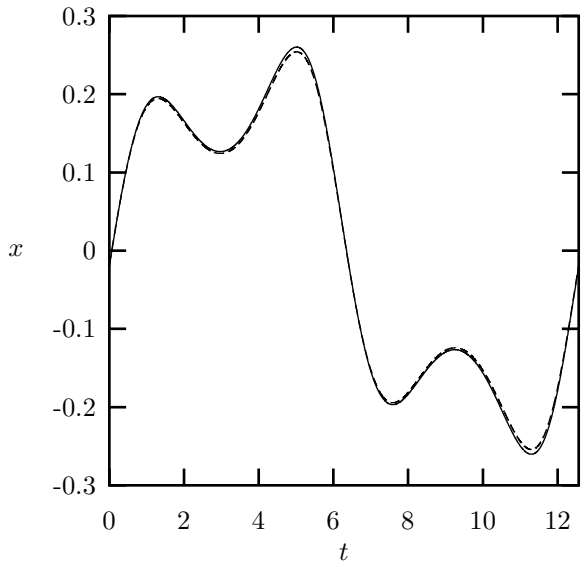

Figure 4. Comparison of numerical and analytical approximations of unstable periodic orbit as a time history. Analytical approximation is dashed, numerical integration is solid. Here $\delta = 0.6305$, $\epsilon = 1.47$ and $A = 0.2542$. $\delta_0 \approx 0.6304$, and $\epsilon_0 \approx 1.4386$.

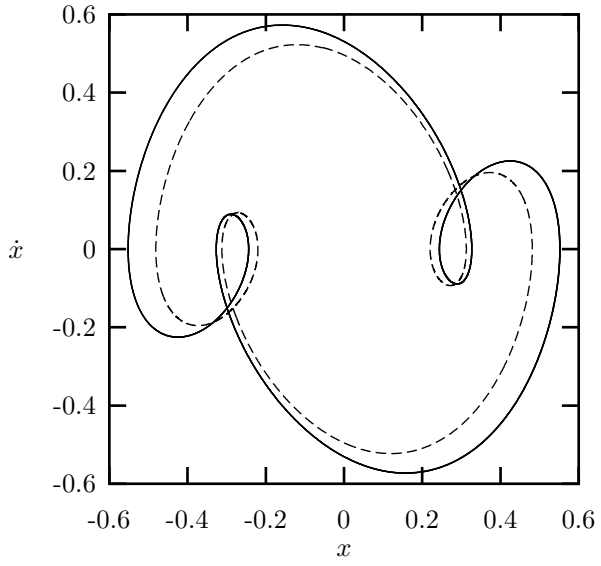

Figure 5. Comparison of numerical and analytical approximations of unstable periodic orbit in the phase plane. Analytical approximation is dashed, numerical integration is solid. Here $\delta = 0.631$, $\epsilon = 1.47$ and $A = 0.2542$. $\delta_0 \approx 0.6304$, and $\epsilon_0 \approx 1.4386$.

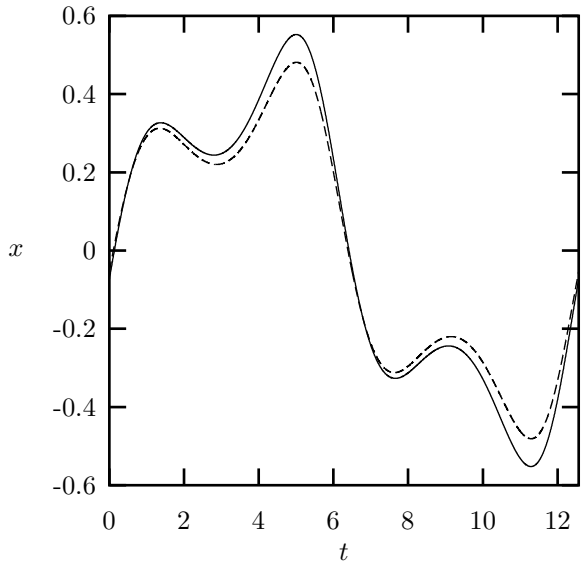

Figure 6. Comparison of numerical and analytical approximations of unstable periodic orbit as a time history. Analytical approximation is dashed, numerical integration is solid. Here $\delta = 0.631$, $\epsilon = 1.47$ and $A = 0.2542$. $\delta_0 \approx 0.6304$, and $\epsilon_0 \approx 1.4386$.

secondary bifurcation curve. We begin by setting up a convenient local coordinate system in parameter space centered at point P, as follows: Note that in Equation (54), the special case of $A = 0$ corresponds to a bifurcation which produces a periodic orbit at the origin. This bifurcation occurs along the transition curve. Therefore, by setting $A = 0$ an expression for the transition curve can be obtained. A natural choice of coordinates is suggested by this observation. The new coordinates are defined by

$$u = \Delta - \left(k_1\epsilon_1^2 + k_3\epsilon_1^3 + k_7\epsilon_1^4 + k_8\epsilon_1^5\right) \tag{55}$$

$$v = \epsilon_1, \tag{56}$$

where $\Delta \equiv \delta - \delta_0$. The coordinate u measures the distance in δ from the transition curve. The coordinate v measures the distance in ϵ from P.

In the new coordinates, Equation (54) takes the form

$$\begin{aligned} u =& vk_{14}A^6 + \left(vk_{11} + v^3k_{12} + k_5\right)A^4 \\ &+ \left(2k_2 + k_4v + k_6v^2 + k_9v^3\right)A^2. \end{aligned} \tag{57}$$

The secondary bifurcation curve can be obtained by noting that Equation (57) generates a series expansion for u in terms of v for small values of A. If the value of v

is fixed – equivalently, if the value of ϵ_1 is fixed – then Equation (57) can be considered to give the value of A as the value of u is varied. Since u is a measure of the distance from the transition curve, this curve gives the dependence of A on δ. For a given value of u there should be two real, positive values of A, corresponding to the two periodic motions (one stable and one unstable) that exist in this region of the parameter plane. The bifurcation occurs when these two motions come together. In terms of the u-A curve, this happens at a vertical tangency in the curve, or when $\frac{du}{dA} = 0$. This condition, along with Equation (57), gives two conditions on u, v, and A. A can be eliminated from these equations, resulting in a single equation between u and v.

Because of the slow convergence of the series in Equation (57), illustrated by Figures 3 – 4 and Figures 5 – 6, directly following the prescription above will not yield the bifurcation curve. Even assuming that the radius of convergence of the series will allow extension to the bifurcation curve, a prohibitive number of terms may be needed to actually obtain satisfactory convergence. **To improve the convergence properties of the power series, Padé approximants are used.** The theory of Padé approximants is discussed in (Bender and Orszag, 1978) and (Rand, 1994). The fundamental idea of Padé summation is to replace a truncated power series by a rational function of polynomials, which has the same Taylor series as the truncated power series.

To apply the method to this problem, Equation (57) is converted to a Padé approximant. For this case, there are three possible approximants

$$u = a^3 b_3 + a^2 b_2 + a b_1 \tag{58}$$

$$u = \frac{-a b_1^3}{a^2 (b_1 b_3 - b_2^2) + a b_1 b_2 - b_1^2} \tag{59}$$

$$u = \frac{a^2 \left(b_1 b_3 - b_2^2\right) - a b_1 b_2}{a b_3 - b_1}, \tag{60}$$

where $a = A^2$, and

$$b_1 = 2k_2 + k_4 v + k_6 v^2 + k_9 v^3 \tag{61}$$

$$b_2 = v k_{11} + v^3 k_{12} + k_5 \tag{62}$$

$$b_3 = v k_{14}. \tag{63}$$

Each of the three approximants needs to be tested individually for good convergence. Of the three, only Equation (59) gives adequate convergence results. By taking the derivative of Equation (59) with respect to a and then eliminating a, substituting the values of the b_i and then the k_i, the following numerical equation relating u and v can be obtained

$$u = 0.01465v + 0.06596v^2. \tag{64}$$

Equation (64) can be written in terms of δ and ϵ by substituting Equation (55). Finally, a relationship between δ and ϵ may be obtained

$$\begin{aligned}\delta = &- 0.00534\epsilon^5 + 0.04716\epsilon^4 - 0.13696\epsilon^3 \\ &+ 0.14908\epsilon^2 + 0.01551\epsilon + 0.58301.\end{aligned} \tag{65}$$

Equation (65) is an approximation to the secondary bifurcation curve.

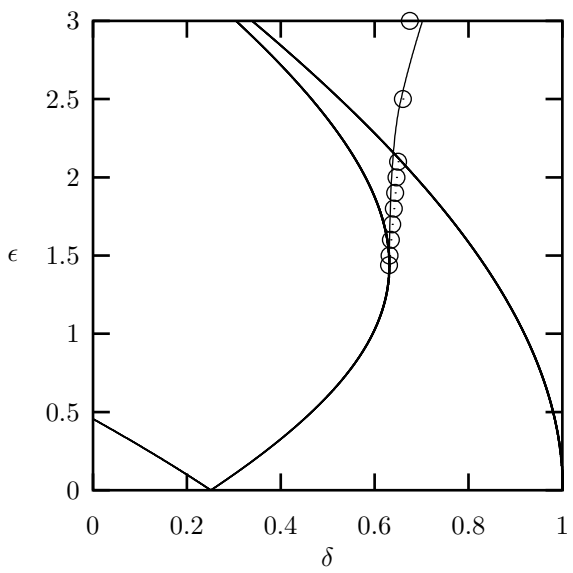

Figure 7. Comparison of analytical and numerical approximation to secondary bifurcation curve. Analytical approximation is the solid line, numerical values are points.

Figure 7 shows the analytical and numerical approximations to the bifurcation curve. The analytical approximation, shown as a solid line, is in close agreement up to $\epsilon = 2.5$, at which point it becomes less reliable. The perturbation method is assumed to be valid in the neighborhood of $\epsilon_0 \approx 1.4386$, so the approximation in Equation (65) is working quite well.

In cases such as the present one, it seems that the bifurcation curve should arise from a tangency with the transition curve. Since the bifurcation is assumed to occur at a point along the transition curve which has a vertical tan-

gency, the bifurcation curve itself is assumed to have a vertical tangency. In the present instance, this is not the case. The analytical expression for the bifurcation curve is nearly vertical, but it is not truly vertical.

CONCLUSIONS

The bifurcations in the quadratically-damped Mathieu equation were studied. Special focus was given to the region of the δ- ϵ parameter plane around point P, the point of infinite slope along the right transition curve of the 2:1 instability region. In this region a bifurcation sequence was numerically identified. It was observed that above P an unstable periodic motion is born by crossing out of the instability region. On the other hand, below P, a stable periodic motion is born by crossing into the instability region. Moreover, a secondary bifurcation curve in which the previously mentioned stable and unstable periodic motions merge, was seen to emanate from point P.

In order to obtain an approximation for this secondary bifurcation, a new approach was developed. This involved perturbing directly off of Mathieu's equation and using Mathieu functions instead of the usual sines and cosines. An interesting feature of this method is its semi-analytical nature. Because Mathieu functions do not have closed-form representations that are easy to manipulate, the method needed to be executed semi-analytically, that is, certain integrals had to be evaluated by numerical quadrature.

When combined with Padé approximants, the perturbation method recovered an acceptable approximation to the secondary bifurcation curve in a neighborhood of point P. In fact, the resulting approximation was seen to be reasonable for values of ϵ up to 2.5, although since the perturbation method itself can be expected to be valid only in a neighborhood of point P, this agreement must be viewed as serendipitous.

ACKNOWLEDGMENT

Author Ramani wishes to acknowledge support for this work in the form of a National Science Foundation Graduate Research Fellowship. This work was partially supported by the Office of Naval Research, Program Officer Dr. Roy Elswick, Code 321.

References

Bender, C. M. and Orszag, S. A. (1978). *Advanced Mathematical Methods For Scientists and Engineers*. McGraw-Hill, Inc., New York.

Nayfeh, A. H. and Mook, D. T. (1979). *Nonlinear Oscillations*. John Wiley & Sons, Inc., New York.

Ramani, D. V. (2001). *The Nonlinear Dynamics Of Towed Array Lifting Devices*. PhD thesis, Cornell University, Ithaca, NY.

Rand, R. H. (1994). *Topics In Nonlinear Dynamics With Computer Algebra*. Gordon and Breach Science Publishers, USA.

Rand, R. H., Ramani, D. V., Keith, W. L., and Cipolla, K. M. (2000b). Theoretical study of a submarine towed-array lifting device. In *Proceedings of the UDT (Undersea Defence Technology) Europe 2000 Conference (CD-ROM)*, June 27–29, 2000, Wembley Conference Center, London, UK.

Rand, R. H., Ramani, D. V., Keith, W. L., and Cipolla, K. M. (2000a). The quadratically damped mathieu equation and its application to submarine dynamics. In Tzou, H., Golnaraghi, M., and Radcliffe, C., editors, *Proceedings of the 2000 ASME International Mechanical Engineering Congress and Exposition*, volume AD-Vol. 61 of *Control of Noise and Vibration: New Millenium*, pages 39–50, Nov. 5–10, 2000, Orlando, FL. ASME.

Stoker, J. (1950). *Nonlinear Vibrations*. Wiley-Interscience, New York.

APPENDIX: DEFINITIONS OF f_i AND g_i

In this appendix we present definitions for the functions in the perturbation method at point P. The method for developing these is given in the text.

$$x_0 = Af_1 \tag{66}$$

$$x_1 = A\epsilon_1 f_2 + A^2 g_1 \tag{67}$$

$$x_2 = A\epsilon_1^2 f_3 + A^2\epsilon_1 g_2 + 2A^3 f_4 \tag{68}$$

$$x_3 = A^2\epsilon_1^2 g_3 + A^4 g_4 + A^3\epsilon_1 f_5 + A\epsilon_1^3 f_6 \tag{69}$$

$$\begin{aligned} x_4 = {} & A\epsilon_1^4 f_7 + A^2\epsilon_1^3 g_5 + A^3\epsilon_1^2 f_8 + A^4\epsilon_1 g_6 \\ & + A^5 f_9 \frac{A^6}{3} f_{10} + \frac{A^3\epsilon_1^3}{3} g_7 \\ & + A^4\epsilon_1^2 f_{11} + A^5\epsilon_1 g_8, \end{aligned} \tag{70}$$

where

$$Lf_1 = 0 \tag{71}$$

$$Lf_2 = -f_1 \cos t \tag{72}$$

$$Lg_1 = -\left|\dot{f}_1\right| \tag{73}$$

$$Lf_3 = -k_1 f_1 - f_2 \cos t \tag{74}$$

$$Lf_4 = -k_2 f_1 - g_1 \left|\dot{f}_1\right| \tag{75}$$

$$Lg_2 = -g_1 \cos t - \dot{f}_2 \left| \dot{f}_1 \right| \tag{76}$$

$$\begin{aligned} Lf_5 = &-k_4 f_1 - 2k_2 f_2 - 2f_4 \cos t \\ &- 2\dot{g}_2 \left| \dot{f}_1 \right| - 2\dot{f}_2 \dot{g}_1 \ \mathrm{sgn} \dot{f}_1 \end{aligned} \tag{77}$$

$$Lf_6 = -k_3 f_1 - k_1 f_2 - f_3 \cos t \tag{78}$$

$$Lf_7 = k_7 f_1 + k_3 f_2 + k_1 f_3 + f_5 \cos t \tag{79}$$

$$\begin{aligned} Lf_8 = &k_6 f_1 + k_4 f_2 + 2k_2 f_3 + 2k_1 f_4 + 2\dot{g}_3 \left| \dot{f}_1 \right| \\ &+ 2\dot{g}_2 \dot{f}_2 \ \mathrm{sgn} \ \dot{f}_1 + 2\dot{g}_1 \dot{f}_3 \ \mathrm{sgn} \ \dot{f}_1 + f_5 \cos t \end{aligned} \tag{80}$$

$$Lf_9 = \dot{g}_1^2 \dot{f}_2 \delta \left(A \dot{f}_1 \right) \tag{81}$$

$$Lf_{10} = -\dot{f}_2^3 \delta \left(A \dot{f}_1 \right) \tag{82}$$

$$Lf_{11} = -\dot{g}_1^2 \dot{f}_2 \delta \left(A \dot{f}_1 \right) \tag{83}$$

$$Lg_3 = -k_1 g_1 - g_2 \cos t - 2\dot{f}_3 \left| \dot{f}_1 \right| - {\dot{f}_2}^2 \ \mathrm{sgn} \dot{f}_1 \tag{84}$$

$$Lg_4 = -2k_2 g_1 - 4\dot{f}_4 \left| \dot{f}_1 \right| - {\dot{g}_1}^2 \ \mathrm{sgn} \dot{f}_1 \tag{85}$$

$$\begin{aligned} Lg_5 = &k_3 g_1 + k_1 g_2 + g_3 \cos t + 2\dot{f}_6 \left| \dot{f}_1 \right| \\ &+ 2\dot{f}_2 \dot{f}_3 \ \mathrm{sgn} \ \dot{f}_1 \end{aligned} \tag{86}$$

$$\begin{aligned} Lg_6 = &k_4 g_1 + 2k_2 g_2 + g_4 \cos t + 2\dot{g}_2 \dot{g}_1 \ \mathrm{sgn} \ \dot{f}_1 \\ &+ 2\dot{f}_5 \left| \dot{f}_1 \right| + 4\dot{f}_4 \dot{f}_2 \ \mathrm{sgn} \ \dot{f}_1 \end{aligned} \tag{87}$$

$$Lg_7 = -\dot{g}_1^3 \delta \left(A \dot{f}_1 \right) \tag{88}$$

$$Lg_8 = -\dot{g}_1 \dot{f}_2^2 \delta \left(A \dot{f}_1 \right) \tag{89}$$